

# Metamorphism obscures primary taphonomic pathways in the early Cambrian Sirius Passet Lagerstätte, North Greenland

Morten Lunde Nielsen<sup>1,2,3</sup>, Mirinae Lee<sup>3</sup>, Hong Chin Ng<sup>1</sup>, Jeremy C. Rushton<sup>2</sup>, Katharine R. Hendry<sup>1</sup>, Ji-Hoon Kihm<sup>3</sup>, Arne T. Nielsen<sup>4</sup>, Tae-Yoon S. Park<sup>3,5</sup>, Jakob Vinther<sup>1</sup> and Philip R. Wilby<sup>2</sup>

<sup>1</sup>School of Earth Sciences, University of Bristol, Bristol BS8 1TQ, UK

<sup>2</sup>British Geological Survey, Keyworth, Nottingham NG12 5GG, UK

<sup>3</sup>Division of Earth Sciences, Korea Polar Research Institute, Yeosu-gu, Incheon 21990, Republic of Korea

<sup>4</sup>Department of Geosciences and Natural Resource Management, University of Copenhagen, 1350 Copenhagen, Denmark

<sup>5</sup>Polar Science, University of Science and Technology, Daejeon 34113, Republic of Korea

## ABSTRACT

**Correct interpretation of soft-bodied fossils relies on a thorough understanding of their taphonomy. While the focus has often been on the primary roles of decay and early diagenesis, the impacts of deeper burial and metamorphism on fossil preservation are less well understood. We document a sequence of late-stage mineral replacements in panarthropod fossils from the Sirius Passet Lagerstätte (North Greenland), an important early Cambrian Burgess Shale-type (BST) biota. Muscle and gut diverticula were initially stabilized by early diagenetic apatite, prior to being pervasively replaced by quartz and then subordinate chlorite, muscovite, and chloritoid during very low- to low-grade metamorphism. Each new mineral replicates the soft tissues with different precision and occurs in particular anatomical regions, imposing strong biases on the biological information retained. Muscovite and chloritoid largely obliterate the tissues' original detail, suggesting that aluminum-rich protoliths may have least potential for conserving mineralized soft tissues in metamorphism. Overall, the fossils exhibit a marked shift toward mineralogical equilibration with the matrix, obscuring primary taphonomic modes. Sequential replacement of the phosphatized soft tissues released phosphorus to form new accessory monazite (and apatite and xenotime), whose presence in other BST biotas might signal the prior, more widespread, occurrence of this primary mode of preservation. Our results provide critical context for interpreting the Sirius Passet biota and for identifying late-stage overprints in other biotas.**

## INTRODUCTION

Burgess Shale-type (BST) biotas provide critical insight into the function of Cambrian marine ecosystems and into the soft-part anatomy of diverse animal stem lineages (e.g., Daley and Edgecombe, 2014). Much progress has been made toward resolving the depositional controls on their occurrence (see Gaines, 2014) and the resulting biases in the view they provide. They are primarily preserved as carbonaceous cuticular compressions (Butterfield, 1990; Gaines et al., 2012), locally augmented by early diagenetic pyrite coatings (e.g., Gabbott et al., 2004). This commonality in preservation has promoted the view that BST biotas

form a coherent taphonomic grouping, the consequence of a complex trade-off between decay, organic stabilization, and early diagenetic mineralization (Schiffbauer et al., 2014; Anderson et al., 2020; Saleh et al., 2021). However, little is known about the impact of deeper burial and very low- to low-grade metamorphism (i.e., anchizone to epizone) on the taphonomic outcome of these biotas. These processes have predictable consequences for the maturation of the carbonaceous fossils (Butterfield, 1990; Topper et al., 2018) and for the mineralogy and texture of their host sediments (e.g., Powell, 2003; Strang et al., 2016b; Lerosey-Aubril et al., 2018), but the extent to which they over-

print primary taphonomic signals or introduce artifacts is unclear.

We combine geochemical and petrographic analyses from scanning electron microscopy and stable silicon isotopes (see the Supplemental Material<sup>1</sup>) to resolve the impact of these processes on the early Cambrian (Series 2, Stage 3) Sirius Passet Lagerstätte (North Greenland), one of the oldest and least well understood BST biotas (Harper et al., 2019). It, like most other BST biotas, is dominated by arthropods but is distinguished by having experienced an unusually high grade of metamorphism, reaching a peak temperature of  $409 \pm 50$  °C (lower greenschist facies) during the Devonian Ellesmerian orogeny (Soper and Higgins, 1987); by comparison, the Burgess Shale (British Columbia, Canada) reached a peak temperature of  $335 \pm 50$  °C (Topper et al., 2018). The occurrence of silicified muscles in this biota (Fig. 1) has led to the hypothesis that an Ediacaran silicification window (Tarhan et al., 2016) continued into the Cambrian, resulting in a unique style of BST preservation (Strang et al., 2016b). However, we show instead that this is a consequence of the Lagerstätte's burial history, which has profoundly altered original fossil preservation. This new understanding provides both a context for interpreting this biota and for recognizing modified primary taphonomic signals in others.

## RESULTS AND INTERPRETATION

The mineralized labile soft tissues of panarthropods are preserved in a diversity of silicate

<sup>1</sup>Supplemental Material. Materials, methods and bulk rock geochemical characterization. Please visit <https://doi.org/10.1130/G48906.1> to access the supplemental material, and contact [editing@geosociety.org](mailto:editing@geosociety.org) with any questions. The supporting petrographic dataset is available at the University of Bristol (UK) Data Repository ([data.bris](https://doi.org/10.5523/bris.1imwjxexzgxu332uqzlna2lugud)) at <https://doi.org/10.5523/bris.1imwjxexzgxu332uqzlna2lugud>

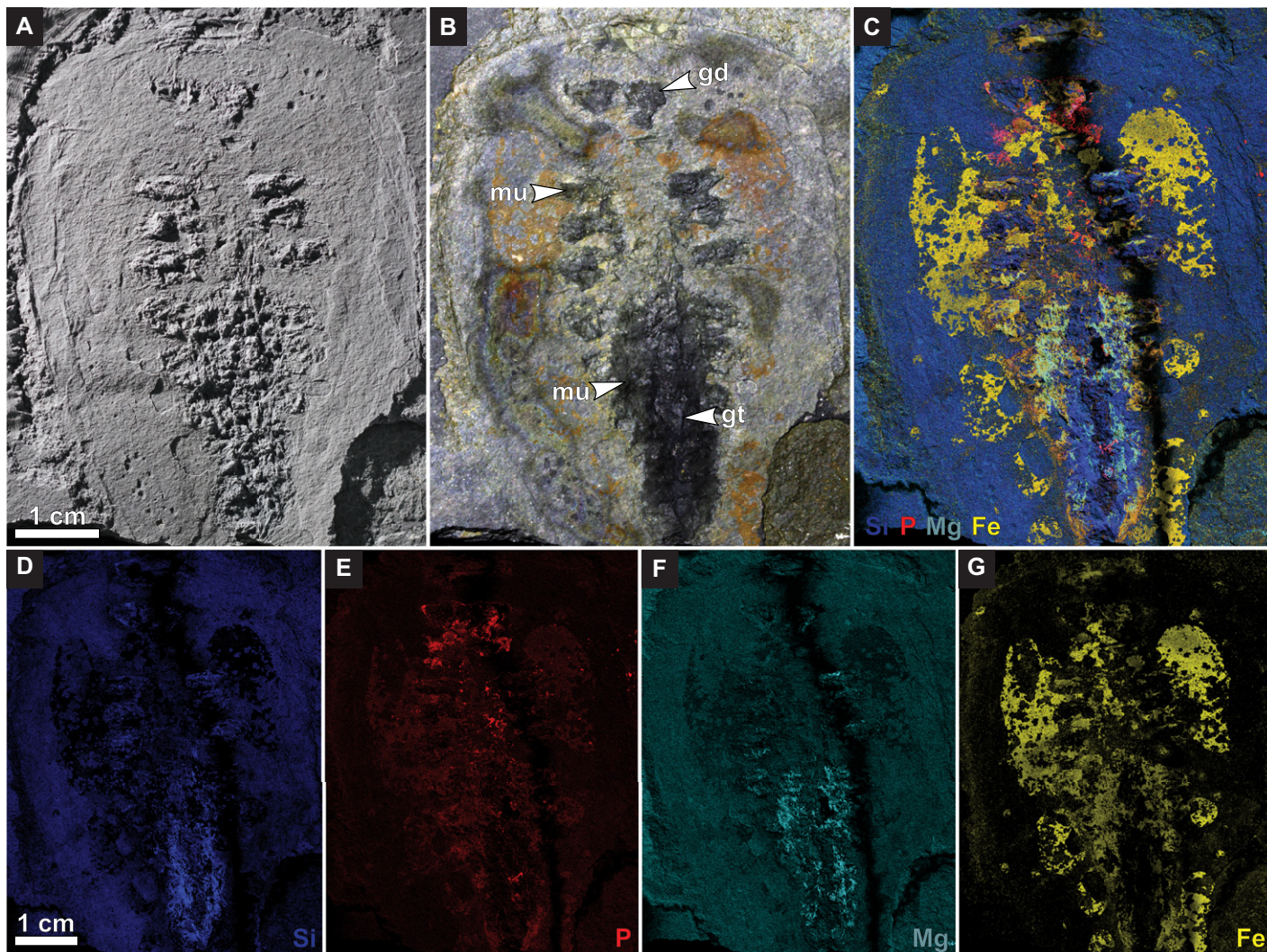
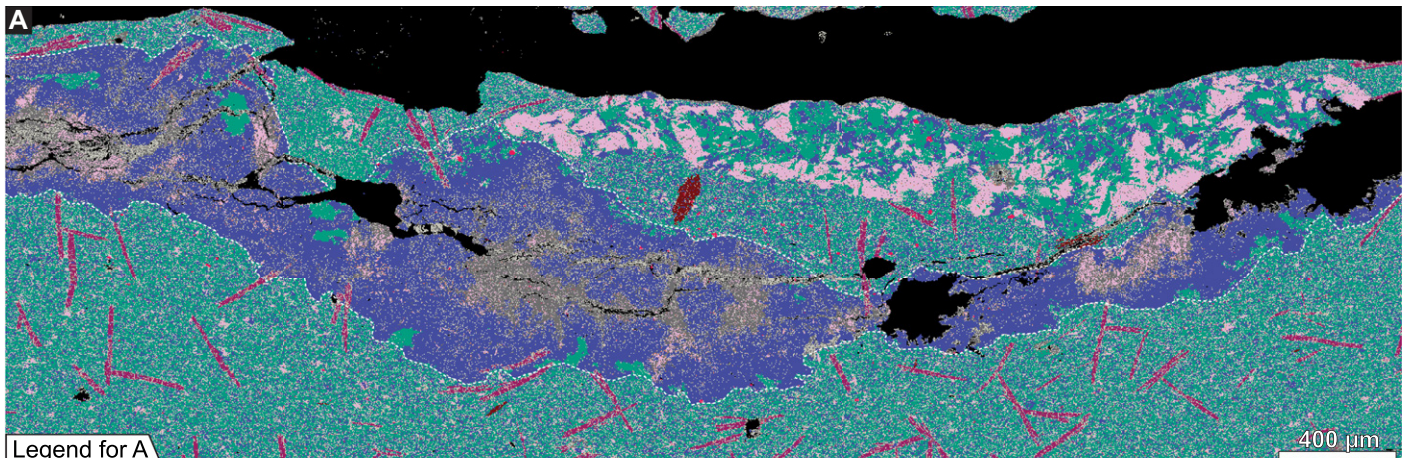


**Figure 1.** Soft-tissue preservation in *?Sidneyia* sp. (Natural History Museum of Denmark specimen MGUH-33947) from the Sirius Passet Lagerstätte (North Greenland). (A,B) Contrasting preservation of compressed exoskeleton and three-dimensional internal anatomy revealed by low-angle light (A), and high-angle light under water (B). Abbreviations: gd—gut diverticula; gt—gut tract; mu—muscle. (C–G) Corresponding energy-dispersive X-ray (EDS) elemental maps, with brightness indicating relative abundance. (C) Composite for silicon (Si), phosphorus (P), magnesium (Mg), and iron (Fe), showing localization of mineral phases. (D) Si map indicating preferential silicification of muscle. (E) P map indicating phosphatization of gut tract and diverticula. (F) Mg map representing chlorite associated with silicified muscle. (G) Fe map indicating partial pyritization of cuticle.

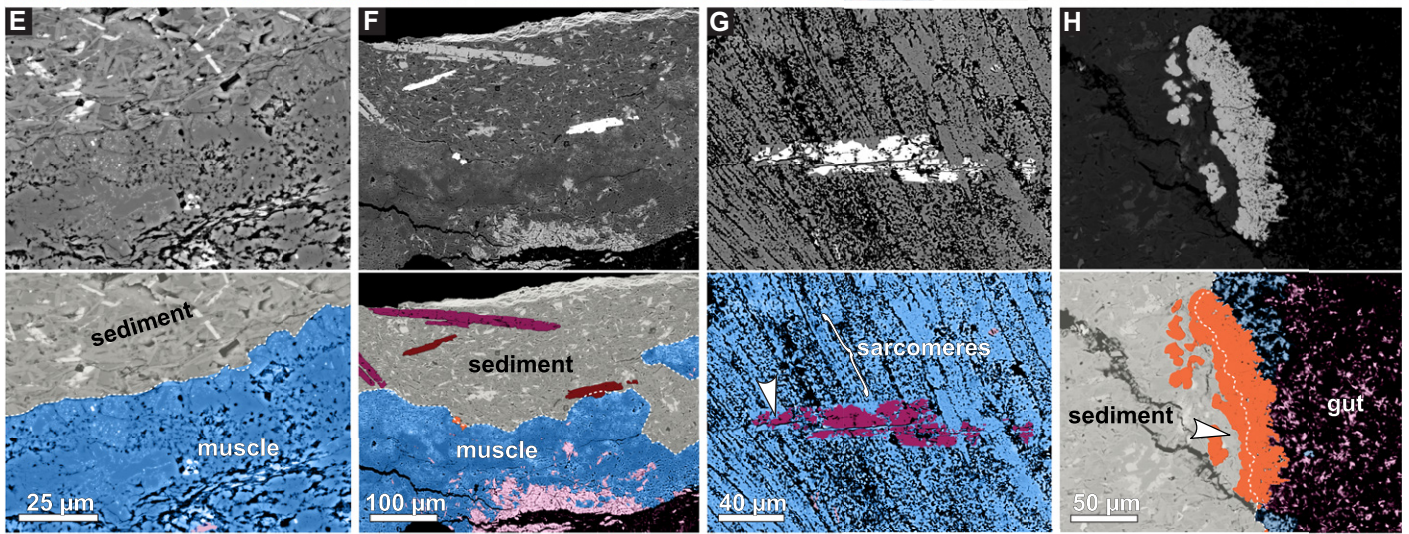
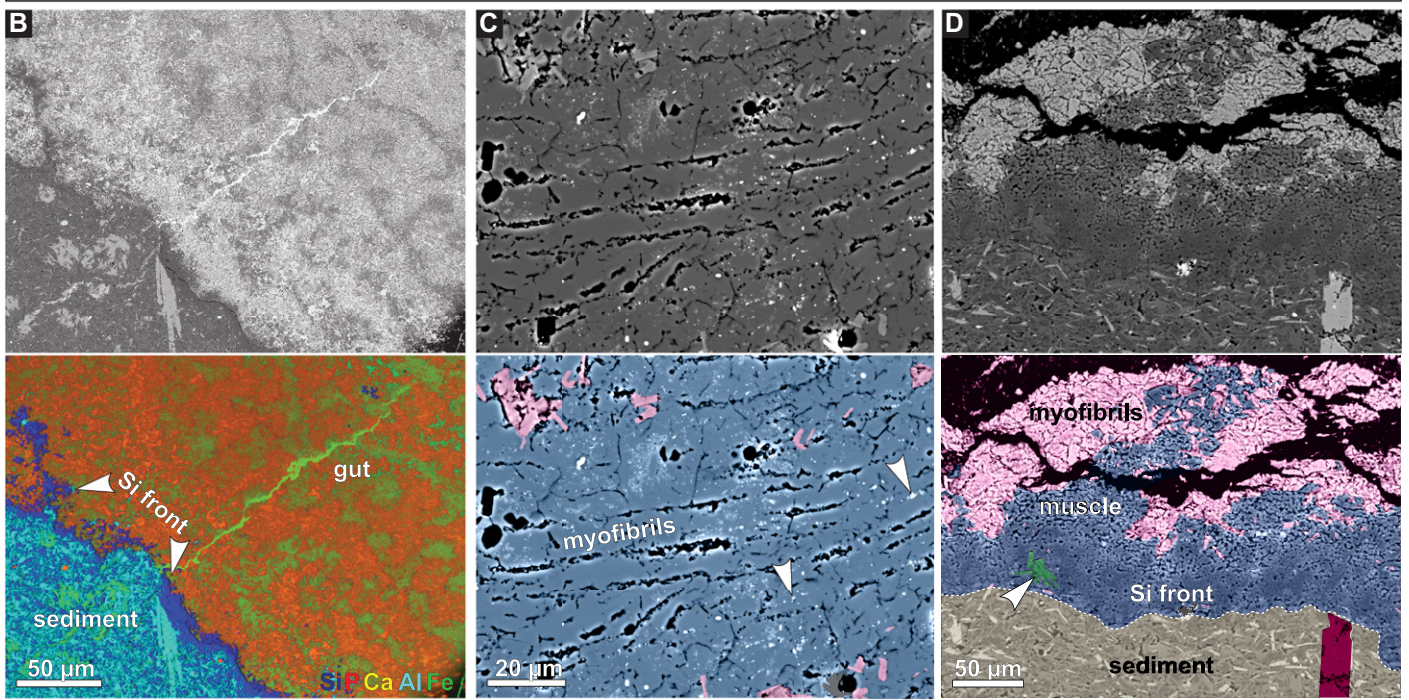
and non-silicate minerals (Figs. 1C and 2A), most shared with the host sediment. Cross-cutting relationships reveal the general paragenetic sequence: apatite > quartz > chlorite  $\pm$  muscovite > chloritoid > xenotime.

Apatite  $[\text{Ca}_5(\text{CO}_3, \text{PO}_4)_3(\text{OH}, \text{F})]$  is invariably the first phase, consistent with its early preservation of soft tissues in other biotas (Briggs et al., 1993). It is extensively replaced by subsequent phases, except in the guts (Fig. 2B) where it frequently remains important. Quartz  $[\text{SiO}_2]$  is the dominant phase (Fig. 2A) and formed in multiple generations, including after late-stage chloritoid (see below; Fig. 2G). However, it everywhere succeeds apatite, as evidenced by abundant relict ( $<1 \mu\text{m}$ ) apatite inclusions (Fig. 2C). Silicification is focused at the margins of the fossils (Figs. 2B and 2D), where inter-

**Figure 2.** Key textural relationships of minerals in sectioned soft tissues from the Sirius Passet Lagerstätte (North Greenland). (A) Energy-dispersive X-ray (EDS) mineral map of transverse section through *?Sidneyia* sp. (Natural History Museum of Denmark specimen MGUH-33942), with extensively silicified musculature and chloritized viscera; chloritoid and monazite are mostly confined to host sediment. (B) Backscattered electron and corresponding wavelength-dispersive spectroscopy (WDS) elemental map of gut diverticula preserved in apatite (P and Ca) against Al-rich sediment with intervening rim of quartz (Si front) (*Arthroaspis bergstroemi*, MGUH-33920). (C–H) BSE images with corresponding false-color overlays. (C) Silicified muscle locally overprinted by chlorite; original preservation in apatite indicated by relict inclusions (arrowed) (*Siriocaris trollae*, MGUH-33945). (D) Muscle preserved by quartz and chlorite; silicification is densest (Si front) against sediment (dotted white line) where patchy muscovite (arrowed) destroys muscle's structure (*?Sidneyia* sp., MGUH-33942). (E) Muscle preserved by microcrystalline quartz, except against sediment (white dotted line) where it is replaced by prismatic inclusion-rich quartz (*?Sidneyia* sp., MGUH-33942). (F) Silicified and chloritized muscle with accessory monazite and xenotime at or near sediment boundary (dotted line) (*?Sidneyia* sp., MGUH-33942). (G) Silicified muscle cross-cut by late-stage chloritoid, which destroys subcellular detail (sarcomeres) and is itself partially replaced by later quartz (arrowed) (*?Sidneyia* sp., MGUH-33936). (H) Xenotime growing inward (partially dendritic) and outward (prismatic) at fossil-sediment junction; intervening cuticle (arrowed), outlined by xenotime, is now preserved by interlocking quartz and muscovite (*Kiisortoqia soperi*, MGUH-33931).



Legend for A  
 Quartz Apatite Chlorite Muscovite Chloritoid Monazite Xenotime Iron oxides Other



Legend for C–H  
 Quartz Apatite-rich quartz Chlorite Muscovite Chloritoid Monazite Xenotime Matrix Other

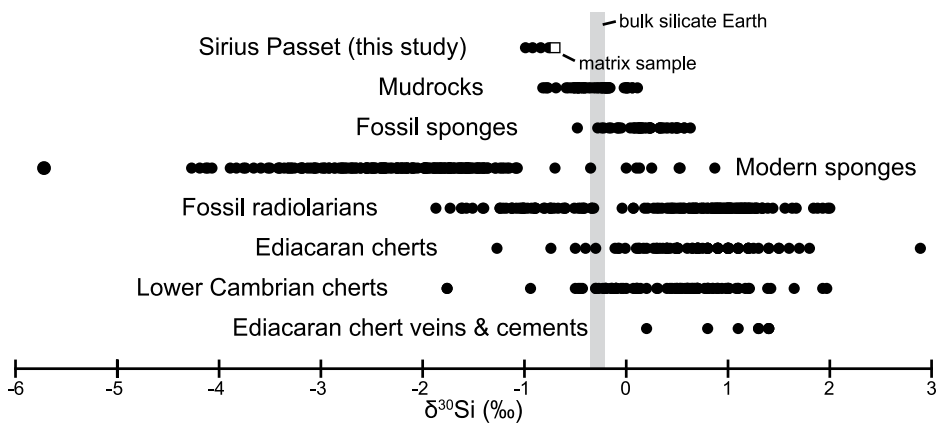


**Figure 3.**  $\delta^{30}\text{Si}$  values for silicified muscle (closed circles) and matrix (open square) samples from the Sirius Passet Lagerstätte (North Greenland) compared to published ranges (see the Supplemental Material [see footnote 1] for references). Minimal variability within Sirius Passet samples and their distinction from alternative potential sources suggest a matrix-derived source for soft-tissue silicification.

locking crystals of quartz ( $\sim 5\text{--}20\ \mu\text{m}$ ) growing inwards from the sediment may obliterate fine morphological detail (Fig. 2E; Fig. S1A in the Supplemental Material). Elsewhere, the quartz is microcrystalline and faithfully replicates subcellular details originally captured by apatite, such as muscle myofibrils (Figs. 2C and 2G). Silicified muscle  $\delta^{30}\text{Si}$  values range between  $-0.76\text{‰}$  and  $-0.99\text{‰}$  (Fig. 3; Table S3), and are notably closer to that of the matrix ( $-0.7\text{‰}$ ) than to other potential contemporary early diagenetic and biogenic low-temperature sources (see Geilert et al., 2014), consistent with a metamorphic origin.

Chlorite [ $(\text{Mg,Fe})_6\text{AlSi}_3\text{O}_{10}(\text{OH})_8$ ] and muscovite [ $\text{KAl}_2(\text{AlSi}_3\text{O}_{10})(\text{OH})_2$ ] typically occur as similarly sized ( $<20\ \mu\text{m}$  long) lath-shaped crystals; locally, they are intergrown, indicating cogenesis. Whereas chlorite is widespread (Fig. 1F) and may faithfully pseudomorph silicified soft tissues (Fig. 2D; Fig. S1B), muscovite is generally confined to discrete domains (Figs. 2A and 2D; Fig. S1C) and does not replicate ultrastructural details. Chloritoid [ $(\text{Fe,Mg,Mn})_2\text{Al}_4\text{Si}_2\text{O}_{10}(\text{OH})_4$ ] principally occurs in the sediment (Fig. 2A) along with pyrite [ $\text{FeS}_2$ ] porphyroblasts (generally  $50\text{--}90\ \mu\text{m}$ ), but it locally overprints silicified muscle and gut diverticula (Fig. S1C), particularly near the fossil margins or adjacent to sediment inclusions. The chloritoid forms large (as much as  $320\ \mu\text{m}$  long) lath-shaped euhedra that traverse multiple muscle fibers and destroy all original morphology (Fig. 2G). Their long axes exhibit a degree of preferred orientation (Fig. S1D), implying growth under stress.

Cuticles typically appear as thin kerogen films (carbon compressions), commonly accompanied by a patchy coating of (now oxidized) pyrite (Figs. 1B and 1G; Fig. S3). However, they may also be preserved by interlocking muscovite and quartz, indistinguishable from the sediment (Fig. 2H).

Accessory phosphate minerals occur in close association with the fossils and overprint the mineralized soft tissues, largely destroying their fine morphology. Xenotime [ $\text{YPO}_4$ ] forms rosettes within the digestive tract, may crudely preserve muscle tissue (Fig. S2D), and locally grows outwards (Figs. S2A–S2C) and inwards from the walls of fossils (Fig. 2H; Figs. S2B and S2C). Similarly, subhedral to euhedral apatite (as large as  $\sim 20\ \mu\text{m}$ ) (Fig. S2G) occurs both inside and outside the fossils, in the latter case as a diffuse corona extending  $\sim 400\ \mu\text{m}$  away (Figs. S2E and S2F). By contrast, monazite [(REE) $\text{PO}_4$ , where REE indicates rare earth elements] is generally confined to the adjacent sediment (Fig. 2F), where it may be concentrated on only one side of fossils (Figs. S2E and S2F), suggesting growth linked to fluid movement (cf. Evans et al., 2002). In all cases, it is poikiloblastic and comparatively coarse ( $30\text{--}380\ \mu\text{m}$ ), locally replacing accessory apatite (Fig. S2H) and at least partially overlapping syntectonic chloritoid formation (Fig. S2I) (see Wilby et al., 2007). Lastly, an amorphous P, Ca, Fe, Al-rich phase, interpreted to be a weathering product of apatite and pyrite, fills interstices in the fossils (Fig. S2J).

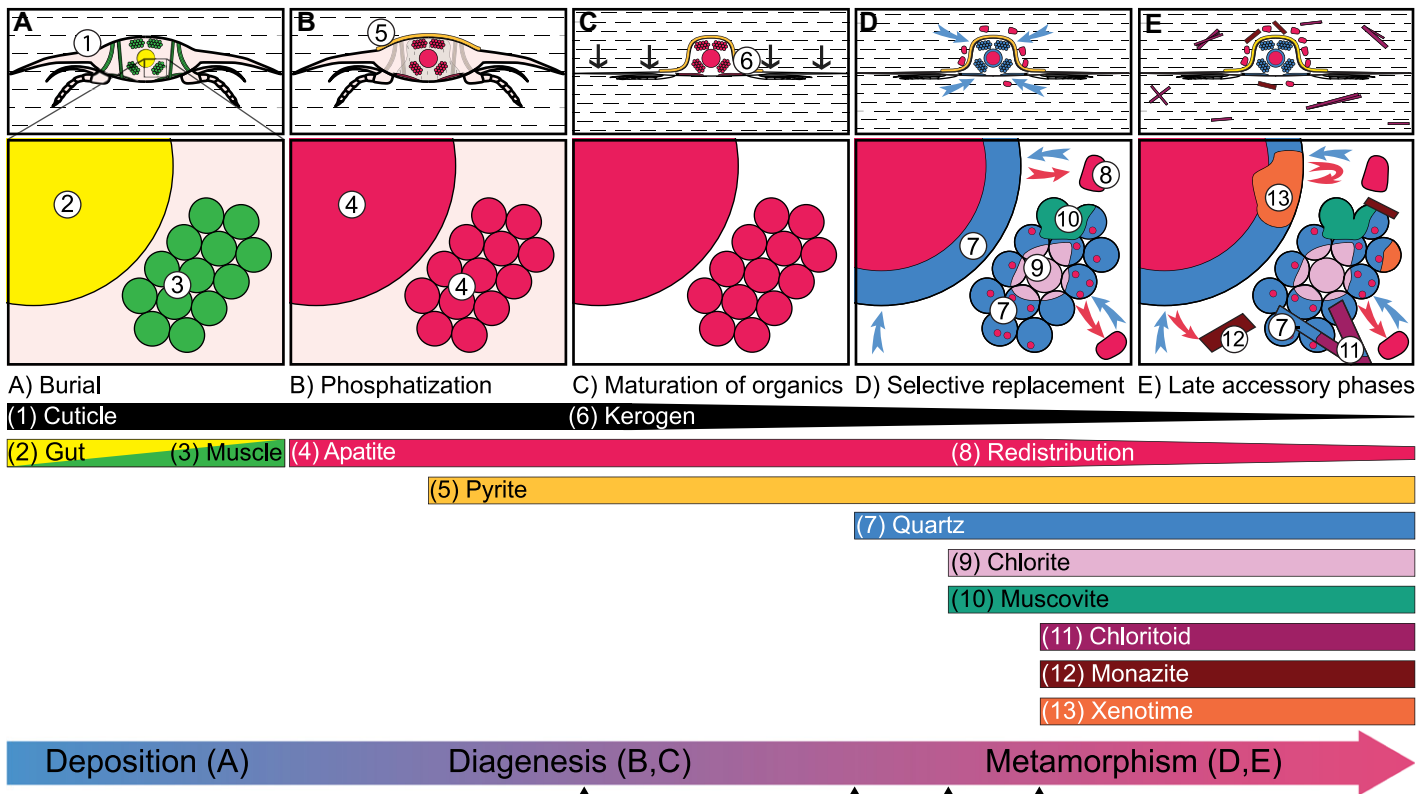
The bulk rock is enriched in aluminum and depleted in calcium compared to the Burgess Shale, but its major element composition otherwise overlaps (for details, see the Supplemental Material; Table S4, Fig. S4). Powell (2003) considered the Burgess Shale to be unremarkable for a pelite, and though the mineralogy of the Sirius Passet protolith cannot be ascertained with certainty (especially the starting clay composition), it likely passed through a typical prograde sequence of mineral reactions for an aluminum-rich pelite (e.g., see Bucher and Grapes, 2011), leading to the observed succession of soft-tissue replacements (Fig. 4).

## DISCUSSION

Silicified soft-bodied biotas are scarce in the Phanerozoic; they rarely preserve labile soft tissues (e.g., muscle) and are confined to exotic non-marine settings (e.g., Trewin et al., 2003). By contrast, early diagenetic silicification was active in diverse marine environments in the Ediacaran and has been implicated in the preservation of several of its soft-bodied biotas (Muscente et al., 2015; Tarhan et al., 2016). This dichotomy has led to the suggestion that a silicification taphonomic window may have persisted into the Cambrian and been responsible for silicifying soft tissues in the Sirius Passet Lagerstätte (Strang et al., 2016a, 2016b; Topper et al., 2018). Our petrographic and isotopic data refute this idea and reveal instead that silicification was a product of very low- to low-grade metamorphism, consistent with its late-stage formation in other BST Lagerstätten (e.g., Powell, 2003; Lerosey-Aubril et al., 2018). Evidence for multiple episodes of silicification in the Sirius Passet Lagerstätte (e.g., before and after chloritoid formation) is consistent with the release of silica from the host sediment during successive clay mineral transformations (van de Kamp, 2008; Fig. 4).

Textural relationships indicate that preserved muscle and digestive systems were initially stabilized by early diagenetic apatite (cf. Wilby et al., 1996; Butterfield, 2002) prior to being progressively replaced by other minerals. Overall, the mineralogy, isotopic composition, and texture of the soft tissues have converged on those of the host sediment, and the primary preservation mode of the soft tissues has been irrevocably altered. Likewise, the originally phosphatized guts have been replaced by quartz and clays, supporting an alternate explanation for apparently sediment-filled guts (Butterfield, 2002), which have been used elsewhere to invoke deposit-feeding habits in certain arthropods (cf. Hou and Bergström, 1997; Lerosey-Aubril et al., 2012). Each new replacing mineral retains a particular level of detail and is focused in discrete anatomical regions (Figs. 1C and 2A), imposing significant biases on the ultimate survival and fidelity of preservation of different tissues. Muscovite and chloritoid growth were especially deleterious, suggesting that aluminum-rich protoliths, such as the Burgess Shale (Powell, 2003), have the least potential for conserving labile soft tissues during very low- to low-grade metamorphism. By contrast, pyrite is unaffected, meaning that this taphonomic pathway at least is reliably conserved (now weathered).

Phosphorus released during successive mineral transformations was redistributed into new accessory phosphates. Accessory monazite is widely reported in other BST biotas (Conway Morris, 1990; Moore and Lieberman, 2009; Broce and Schiffbauer, 2017), implying that phosphatized soft tissues may have been lost



### Mineral reactions:

Protolith: "clays" + Qtz + Kfs + Fe<sub>HR</sub> + C + detritals

I) Kao + Qtz = Prl + water

II) "clays" + Kfs ± Kao = Ill + Qtz + water

IIIa) "clays" + Fe<sub>HR</sub> = Chl + water

IIIb) Ill + Kfs = Ms + Qtz

IVa) Prl + Chl = Cld + Qtz + water

IVb) Ap + REE("clays" ± C) = Mnz

IVc) Ap + Y("clays" ± detritals) = Xn

**Figure 4.** Schematic explanation of key stages (A–E) in preservation of Sirius Passet Lagerstätte (North Greenland) fossils, and postulated pathways for relevant mineral transformations. (A) At burial, prior to decay of cuticle and labile soft tissues (gut and muscle). (B) Phosphatization of labile soft tissues and organic conservation and light pyritization of cuticle. (C) Partial compaction, start of progressive maturation of organics, and transformation of clays. (D) Selective replacement of phosphatized soft tissues by quartz, with concomitant release of phosphorus to pore fluids. Silicified soft tissues undergo progressive replacement by chlorite and muscovite during sediment recrystallization. (E) Precipitation of accessory phosphate minerals at reaction fronts and growth of chloritoid under strain. Quartz continues to precipitate in response to ongoing mineral transformations. The tapering of apatite and kerogen bars illustrate their progressive loss during diagenesis and metamorphism. Abbreviations: Ap—apatite; C—organic carbon; Chl—chlorite; Cld—chloritoid; Fe<sub>HR</sub>—highly reactive iron; detritals—heavy detrital minerals; Ill—illite; Kao—kaolinite; Kfs—K-feldspar; Mnz—monazite; Ms—muscovite; Prl—pyrophyllite; Qtz—quartz; REE—rare earth elements; Xn—xenotime; Y—yttrium; "clays"—refers to presumed composition of deposited clays and micas (smectite, kaolinite, chlorite, and biotite).

from these too and have been a more important component of BST preservation than their present distribution suggests (Daley and Edgecombe, 2014; Paterson et al., 2015). The sum of evidence, including other examples of late-stage overprint (e.g., Gaines et al. 2019), demonstrates the potential for deep burial and metamorphism to modify primary taphonomic signals and biological information, and emphasizes the need for site-specific characterization of the BST preservation.

### CONCLUSIONS

Silicified soft tissues in the Sirius Passet Lagerstätte are a product of progressive altera-

tion of originally phosphatized soft tissues during very low- to low-grade metamorphism. Contrary to previous assertions, they do not record a novel mode of primary BST preservation, but rather an extreme example of a spectrum of late-stage processes that operated in other BST Lagerstätten. The mineralogy and chemistry of Sirius Passet fossils have converged on those of the host sediment, preferentially destroying certain tissues and inducing a reduction in resolution of others. Growth of muscovite and chloritoid was especially destructive, suggesting that protolith composition has a bearing on the ultimate fate of soft tissues during metamorphism. Accessory monazite formed in response to the replacement

of the originally phosphatized soft tissues and may serve as a useful proxy for the former presence of such tissues elsewhere.

### ACKNOWLEDGMENTS

We thank Stuart Kearns (University of Bristol, UK) and Sebastian Næsby Malkki (Geological Survey of Denmark and Greenland) for assistance with electron microscopy, and three anonymous reviewers for helpful suggestions. M.L. Nielsen was supported by a UK Natural Environment Research Council GW4+ Ph.D. studentship (grant NE/L002434/1) with CASE-partner British Geological Survey and a Korea Polar Research Institute (KOPRI) Arctic Science Fellowship Program 2018 grant. J. Rushton and P. Wilby publish with the permission of the Executive Director, British Geological Survey. K. Hendry and H. Ng are supported by a

European Research Council grant ICY-LAB (678371). This work was funded by a Korea Polar Research Institute (KOPRI) project “Advancement into unexplored areas of North Greenland through paleoenvironment and animal evolution research (PE21060)”.

## REFERENCES CITED

- Anderson, R.P., Tosca, N.J., Saupe, E.E., Wade, J., and Briggs, D.E.G., 2020, Early formation and taphonomic significance of kaolinite associated with Burgess Shale fossils: *Geology*, v. 49, p. 355–359, <https://doi.org/10.1130/G48067.1>.
- Briggs, D.E.G., Kear, A.J., Martill, D.M., and Wilby, P.R., 1993, Phosphatization of soft-tissue in experiments and fossils: *Journal of the Geological Society*, v. 150, p. 1035–1038, <https://doi.org/10.1144/gsjgs.150.6.1035>.
- Broce, J.S., and Schiffbauer, J.D., 2017, Taphonomic analysis of Cambrian vermiform fossils of Utah and Nevada, and implications for the chemistry of Burgess Shale-type preservation: *Palaios*, v. 32, p. 600–619, <https://doi.org/10.2110/palo.2017.011>.
- Bucher, K., and Grapes, R., 2011, *Petrogenesis of Metamorphic Rocks*: Berlin, Springer-Verlag, <https://doi.org/10.1007/978-3-540-74169-5>.
- Butterfield, N.J., 1990, Organic preservation of non-mineralizing organisms and the taphonomy of the Burgess Shale: *Paleobiology*, v. 16, p. 272–286, <https://doi.org/10.1017/S0094837300009994>.
- Butterfield, N.J., 2002, *Leaenchoilia* guts and the interpretation of three-dimensional structures in Burgess Shale-type fossils: *Paleobiology*, v. 28, p. 155–171, [https://doi.org/10.1666/0094-8373\(2002\)028<0155:LGA TIO>2.0.CO;2](https://doi.org/10.1666/0094-8373(2002)028<0155:LGA TIO>2.0.CO;2).
- Conway Morris, S., 1990, Burgess Shale, in Briggs, D.E.G. and Crowther, P.R. eds., *Paleobiology: A Synthesis*: Oxford, UK, Blackwell Scientific Publications, p. 270–274.
- Daley, A.C., and Edgecombe, G.D., 2014, Morphology of *Anomalocaris canadensis* from the Burgess Shale: *Journal of Paleontology*, v. 88, p. 68–91, <https://doi.org/10.1666/13-067>.
- Evans, J.A., Zalasiewicz, J.A., Fletcher, I., Rasmussen, B., and Pearce, N.J.G., 2002, Dating diagenetic monazite in mudrocks: Constraining the oil window?: *Journal of the Geological Society*, v. 159, p. 619–622, <https://doi.org/10.1144/0016-764902-066>.
- Gabbott, S.E., Hou, X.G., Norry, M.J., and Siveter, D.J., 2004, Preservation of Early Cambrian animals of the Chengjiang biota: *Geology*, v. 32, p. 901–904, <https://doi.org/10.1130/G20640.1>.
- Gaines, R.R., 2014, Burgess Shale-type preservation and its distribution in space and time, in Laffamme, M., et al., eds., *Reading and Writing of the Fossil Record: Preservation Pathways to Exceptional Fossilization: The Paleontological Society Papers*, v. 20, p. 123–146, <https://doi.org/10.1017/S1089332600002837>.
- Gaines, R.R., Hammarlund, E.U., Hou, X., Qi, C., Gabbott, S.E., Zhao, Y., Peng, J., and Canfield, D.E., 2012, Mechanism for Burgess Shale-type preservation: Proceedings of the National Academy of Sciences of the United States of America, v. 109, p. 5180–5184, <https://doi.org/10.1073/pnas.1111784109>.
- Gaines, R.R., Lombardo, A.J., Holzer, I.O., and Caron, J.B., 2019, The limits of Burgess Shale-type preservation: Assessing the evidence for preservation of the blood protein hemocyanin in the Burgess Shale: *Palaios*, v. 34, p. 291–299, <https://doi.org/10.2110/palo.2019.026>.
- Geilert, S., Vroon, P.Z., Roerdink, D.L., Van Cappellen, P., and van Bergen, M.J., 2014, Silicon isotope fractionation during abiotic silica precipitation at low temperatures: Inferences from flow-through experiments: *Geochimica et Cosmochimica Acta*, v. 142, p. 95–114, <https://doi.org/10.1016/j.gca.2014.07.003>.
- Harper, D.A.T., Hammarlund, E.U., Topper, T.P., Nielsen, A.T., Rasmussen, J.A., Park, T.-Y.S., and Smith, M.P., 2019, The Sirius Passet Lagerstätte of North Greenland: A remote window on the Cambrian Explosion: *Journal of the Geological Society*, v. 176, p. 1023–1037, <https://doi.org/10.1144/jgs2019-043>.
- Hou, X., and Bergström, J., 1997, Arthropods of the Lower Cambrian Chengjiang Fauna, Southwest China: *Fossils and Strata*, v. 45, 116 p.
- Lerosey-Aubril, R., Hegna, T.A., Kier, C., Bonino, E., Habersetzer, J., and Carré, M., 2012, Controls on gut phosphatization: The trilobites from the Weeks Formation Lagerstätte (Cambrian; Utah): *PLoS One*, v. 7, e32934, <https://doi.org/10.1371/journal.pone.0032934>.
- Lerosey-Aubril, R., Gaines, R.R., Hegna, T.A., Ortega-Hernández, J., Van Roy, P., Kier, C., and Bonino, E., 2018, The Weeks Formation Konservat-Lagerstätte and the evolutionary transition of Cambrian marine life: *Journal of the Geological Society*, v. 175, p. 705–715, <https://doi.org/10.1144/jgs2018-042>.
- Moore, R.A., and Lieberman, B.S., 2009, Preservation of early and Middle Cambrian soft-bodied arthropods from the Pioche Shale, Nevada, USA: *Palaeogeography, Palaeoclimatology, Palaeoecology*, v. 277, p. 57–62, <https://doi.org/10.1016/j.palaeo.2009.02.014>.
- Muscente, A.D., Hawkins, A.D., and Xiao, S., 2015, Fossil preservation through phosphatization and silicification in the Ediacaran Doushantuo Formation (South China): A comparative synthesis: *Palaeogeography, Palaeoclimatology, Palaeoecology*, v. 434, p. 46–62, <https://doi.org/10.1016/j.palaeo.2014.10.013>.
- Paterson, J.R., García-Bellido, D.C., Jago, J.B., Gehling, J.G., Lee, M.S.-Y., and Edgecombe, G.D., 2015, The Emu Bay Shale Konservat-Lagerstätte: A view of Cambrian life from East Gondwana: *Journal of the Geological Society*, v. 173, p. 1–11, <https://doi.org/10.1144/jgs2015-083>.
- Powell, W., 2003, Greenschist-facies metamorphism of the Burgess Shale and its implications for models of fossil formation and preservation: *Canadian Journal of Earth Sciences*, v. 40, p. 13–25, <https://doi.org/10.1139/e02-103>.
- Saleh, F., et al., 2021, Insights into soft-part preservation from the Early Ordovician Fezouata Biota: *Earth-Science Reviews*, v. 213, 103464, <https://doi.org/10.1016/j.earscirev.2020.103464>.
- Schiffbauer, J.D., Xiao, S., Cai, Y., Wallace, A.F., Hua, H., Hunter, J., Xu, H., Peng, Y., and Kaufman, A.J., 2014, A unifying model for Neoproterozoic–Palaeozoic exceptional fossil preservation through pyritization and carbonaceous compression: *Nature Communications*, v. 5, 5754, <https://doi.org/10.1038/ncomms6754>.
- Soper, N.J., and Higgins, A.K., 1987, A shallow detachment beneath the North Greenland fold belt: Implications for sedimentation and tectonics: *Geological Magazine*, v. 124, p. 441–450, <https://doi.org/10.1017/S0016756800017027>.
- Strang, K.M., Armstrong, H.A., and Harper, D.A.T., 2016a, Minerals in the gut: Scoping a Cambrian digestive system: *Royal Society Open Science*, v. 3, 160420, <https://doi.org/10.1098/rsos.160420>.
- Strang, K.M., Armstrong, H.A., Harper, D.A.T., and Trabucho-Alexandre, J.P., 2016b, The Sirius Passet Lagerstätte: Silica death masking opens the window on the earliest matground community of the Cambrian explosion: *Lethaia*, v. 49, p. 631–643, <https://doi.org/10.1111/let.12174>.
- Tarhan, L.G., Hood, A.V.S., Droser, M.L., Gehling, J.G., and Briggs, D.E.G., 2016, Exceptional preservation of soft-bodied Ediacara Biota promoted by silica-rich oceans: *Geology*, v. 44, p. 951–954, <https://doi.org/10.1130/G38542.1>.
- Topper, T.P., Greco, F., Hofmann, A., Beeby, A., and Harper, D.A.T., 2018, Characterization of kerogenous films and taphonomic modes of the Sirius Passet Lagerstätte, Greenland: *Geology*, v. 46, p. 359–362, <https://doi.org/10.1130/G39930.1>.
- Trewin, N.H., Fayers, S.R., and Kelman, R., 2003, Subaqueous silicification of the contents of small ponds in an Early Devonian hot-spring complex, Rhynie, Scotland: *Canadian Journal of Earth Sciences*, v. 40, p. 1697–1712, <https://doi.org/10.1139/e03-065>.
- van de Kamp, P.C., 2008, Smectite-illite-muscovite transformations, quartz dissolution, and silica release in shales: *Clays and Clay Minerals*, v. 56, p. 66–81, <https://doi.org/10.1346/CCMN.2008.0560106>.
- Wilby, P.R., Briggs, D.E.G., and Riou, B., 1996, Mineralization of soft-bodied invertebrates in a Jurassic metalliferous deposit: *Geology*, v. 24, p. 847–850, [https://doi.org/10.1130/0091-7613\(1996\)024<0847:MOSBII>2.3.CO;2](https://doi.org/10.1130/0091-7613(1996)024<0847:MOSBII>2.3.CO;2).
- Wilby, P.R., Page, A.A., Zalasiewicz, J.A., Milodowski, A.E., Williams, M., and Evans, J.A., 2007, Syn-tectonic monazite in low-grade mudrocks: A potential geochronometer for cleavage formation?: *Journal of the Geological Society*, v. 164, p. 53–56, <https://doi.org/10.1144/0016-76492006-035>.

Printed in USA